Adaptive Fuzzy Sliding Mode Control of Linear Induction Motors with Unknown End Effect Consideration

Chin-I Huang, Kou-Cheng Hsu, Hsin-Han Chiang, Kuang-Yang Kou, and Tsu-Tian Lee

Abstract—In this paper, an adaptive fuzzy sliding mode controller (AFSMC) is proposed for a linear induction motor (LIM) taking into account the longitudinal end effect and uncertainties including the friction force. The dynamic mathematical model of an indirect field-oriented LIM drive is firstly derived for controlling the LIM. On the basis of a backstepping control law, a sliding mode controller (SMC) embedded with fuzzy boundary layer is designed to compensate lumped uncertainties during the tracking control of periodic reference trajectories. Since the bound of lumped uncertainties is difficult to obtain advance in practical applications, an adaptive tuner based on the sense of Lyapunov stability theorem is derived to adjust the controller parameter in real-time, and also for further confronting the increasing disturbance and uncertainties. The indirect field-oriented LIM with the proposed AFSMC assures the system stability, asymptotic output tracking, and the robust control performance. The effectiveness of the proposed control scheme is verified through experimental results, and its advantages of control performance and robustness are exhibited in comparison with SMC and FSMC approaches.

I. INTRODUCTION

THE linear induction motor (LIM) has been widely used for many years in many industrial applications, such as actuators, transportation, and conveyor systems, due to its robust, cheap, and easily maintained. Compared to the indirect drives that use rotational electrical motors and coupling mechanisms, the LIM exhibits the feature of contactless transfer of electrical power to translational mechanical power. The electromagnetic thrust is applied directly to the payload without the intervention of a mechanical transmission. However, there exists strong interaction between the machine process and the direct drive of the LIM, that is, system friction force and the primary end effect of LIM. The designed principle of controller must include high tracking performance and high dynamic stiffness [1-6].

To deal with such uncertainties, many studies have been done in recent years to apply various approaches in the control field. Among them, sliding mode control (SMC) is

one of the powerful approaches to control nonlinear and uncertain systems [7, 8]. However, it is difficult to obtain the bound of lumped uncertainty in advance for practical applications of SMC. Besides, the disadvantage exists in the application of SMC system is the undesired chattering phenomena which raises imperfection for practical switching device using.

Fuzzy systems have supplanted conventional technologies in many applications, especially in control systems. One major feature of fuzzy logic is its ability to express the amount of ambiguity in human thinking. If the mathematical model of the process does not exist, or exists but with uncertainties, fuzzy logic is an alternative way to deal with the unknown process [9, 10]. However, large amount of fuzzy sets makes the system operation complex for a high-order system. Nowadays, many researchers have tended to combine with fuzzy logic and SMC. The main advantage of fuzzy logic controller design based on SMC is that the number of fuzzy rules can be reduced, and the conservative requirement of the uncertainty bound can be relaxed. Wong *et al.* proposed a fuzzy-based combining controller to remedy the chattering phenomena [11, 12]. However, the parameters of membership functions of this fuzzy controller cannot be adjusted to afford optimal control efforts under the increasing of uncertainty. Such the mentioned problems will be solved in this paper.

In this paper, an adaptive fuzzy sliding mode controller (AFSMC), based on indirect field-oriented LIM model considering with the unknown end effect, is proposed. By using the derived the LIM model, moreover, the proposed controller is applied to achieve position tracking objective under parameter uncertainties and external disturbance.

II. INDIRECT FILED-ORIENTED LIM AND END EFFECT

The primary of the LIM has a finite length, so that there is a fringing field at both ends of the primary. The infinite long secondary enters the air-gap field, carries the magnetic flux along with it, and makes the distribution of the electromagnetic quantities non-uniform. It thus results in considerable electric and force losses [2]. These losses become relevant as the mover speed increases, and this phenomenon is called "end effect."

The primary (mover) is simply a cut open and rolled flat rotary-motor primary. The secondary consists of a sheet conductor using aluminum with an iron back for the return path of magnetic flux. In a LIM, the primary voltage or

Chin-I Huang, Kou-Cheng Hsu, Hsin-Han Chiang are with the Electrical Engineering Department, Fu Jen Catholic University, New Taipei City, Taiwan, ROC (e-mail: hsinhan@ee.fju.edu.tw).

Kuang-Yang Kou is with the Department of Traffic Science, National Central Police University, Taoyuan, Taiwan, ROC (e-mail: peterkou@mail.cpu.edu.tw).

Tsu-Tian Lee is with the Electrical Engineering Department, National Taipei University of Technology, Taipei, Taiwan, ROC (e-mail: ttlee@ntut.edu.tw).
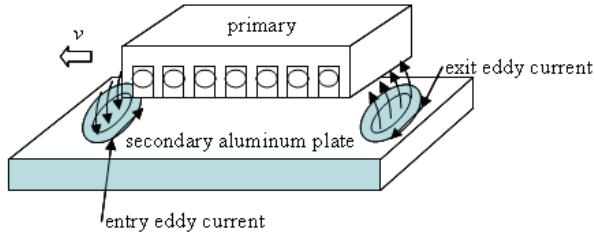
Fig. 1. Eddy-current generation at the entry and exit of the airgap while the primary moves with speed.

current excitation produces a magnetic field, which moves from the front to the back of the primary. This magnetic field induces currents in the conducting layer on the surface of the secondary, which produces a second traveling magnetic field. The interaction of these two magnetic fields produces a force which tends to move the primary along the surface of the secondary sheet. Figure 1 shows a conceptual construction of a LIM.

The mathematical model of LIM is conventionally constructed in "three-phase" parameters. It is really complex to analyze, so we apply a *d-q* axis equivalent circuit to transform the IM's model. By using the fifth order model of LIM [3-5], the voltage equations in the *d-q* axis reference frame aligned with the secondary flux are given as:

$$v_{ds} = R_s i_{ds} + \frac{d}{dt}\lambda_{qs} - \omega_e \lambda_{qs} \qquad (1)$$

$$v_{qs} = R_s i_{qs} + \frac{d}{dt}\lambda_{qs} + \omega_e \lambda_{qs} \qquad (2)$$

$$v_{dr} = R_r i_{dr} + \frac{d}{dt}\lambda_{dr} = 0 \qquad (3)$$

$$v_{qr} = R_r i_{dr} + \frac{d}{dt}\lambda_{qr} = 0 \qquad (4)$$

where (v_{ds}, v_{qs}), (i_{ds}, i_{qs}), and $(\lambda_{ds}, \lambda_{qs})$ are the *d-q* axis voltages, currents and flux linkages of the primary, and (v_{dr}, v_{qr}), (i_{dr}, i_{qr}), and $(\lambda_{dr}, \lambda_{qr})$ are *d-q* axis voltages, currents and fluxes of the secondary in the secondary frame. The flux linkages of the primary and secondary are given by the following:

$$\lambda_{ds} = L_{ls}i_{ds} + L_m(1 - f(Q))(i_{ds} + i_{dr}) \qquad (5)$$
$$\lambda_{qs} = L_{ls}i_{qs} + L_m(1 - f(Q))(i_{qs} + i_{qr}) \qquad (6)$$
$$\lambda_{dr} = L_{lr}i_{dr} + L_m(1 - f(Q))(i_{ds} + i_{dr}) \qquad (7)$$
$$\lambda_{qr} = L_{lr}i_{qr} + L_m(1 - f(Q))(i_{qs} + i_{qr}) \qquad (8)$$

where $Q = lR_r / L_r v$ and $f(Q) = (1 - e^{-Q})/Q$. The electrical thrust force is expressed as:

$$F_e = \frac{3}{2}\frac{n_p \pi}{h}\frac{L_m(1 - f(Q))}{L_r - L_m f(Q)}(\lambda_{dr}i_{qs} - \lambda_{qr}i_{dr}) \qquad (9)$$

$$= M\dot{v} + Dv + F_l$$

In ideally field-oriented control, the secondary flux linkage axis is forced to align with the d-axis, and one can assume that:

$$\lambda_{qr} = \dot{\lambda}_{qr} = 0 \qquad \lambda_{dr} = \text{constant}$$

Now that (3) and (4) can be rearranged as

$$i_{dr} = -\frac{\dot{\lambda}_{dr}}{R_r} \qquad (10)$$

$$i_{qr} = -\frac{\dot{\lambda}_{qr}}{R_r} \qquad (11)$$

Replacing (10) and (11) into (7) and (8), respectively, the following equations can be obtained:

$$\dot{\lambda}_{dr} = k_1 i_{ds} + k_2 \lambda_{dr} \qquad (12)$$
$$\dot{\lambda}_{qr} = k_1 i_{qs} + k_2 \lambda_{qr} \qquad (13)$$

where

$$k_1 = \frac{R_r L_m(1 - f(Q))}{L_m(1 - f(Q)) + L_{lr}}$$

$$k_2 = \frac{R_r}{L_m(1 - f(Q)) + L_{lr}}$$

By using the indirect field-oriented control technique and the fact that electrical time constant is much smaller than the mechanical time constant, from (12) one can obtain that $\dot{\lambda}_{dr} = k_1 i_{ds} + k_2 \lambda_{dr} \approx 0$. After simplifying the electrical thrust force, the following equation can be resulted:

$$F_e = K_f i_{qs} = M\dot{v} + Dv + (F_l + f(v)) \qquad (14)$$

where

$$K_f = \frac{3}{2}\frac{n_p \pi}{h}\frac{L_m^2 [1 - f(Q)]^2}{L_{lr} + L_m[1 - f(Q)]}i_{ds}$$

and the friction force is presented by:

$$f(v) = F_C \,\text{sgn}(v) + (F_S - F_C)e^{-(v/v_s)^2}\,\text{sgn}(v) + K_v v$$

Accordingly, (14) can be reformulated as follows:

$$\dot{v} = -\frac{D}{M}v + \frac{K_f}{M}i_{qs} - \frac{[F_l + f(v)]}{M} \qquad (15)$$

With parameter variations and external load disturbance, the actual LIM driver system can be considered as follows:

$$\dot{d}_m = x$$
$$\dot{x} = (\bar{A}_m + \Delta A)x + (\bar{B}_m + \Delta B)u + F_{do}$$
$$y = d_m \qquad (16)$$

where d_m and v represent the mover position and velocity, respectively. $\bar{A}_m = -M/D$ and $\bar{B}_m = K_F/M$ both are nominal condition parameters; ΔA and ΔB denote the uncertainties of system parameters M and D; $u = i_{qs}$ is the control input to the motor drive system; F_{do} is system uncertainties of friction force and disturbance. The electrical thrust of IM drive system can be reformulated as follow:

$$\dot{x} = \bar{A}_m x + \bar{B}_m u + F_d \qquad (17)$$

where F_d is the lumped uncertainty defined as:

$$F_d = \Delta A x + \Delta B u + F_{do}$$

Here, the control objective is to drive the mover position *y* to track the given reference trajectory y^*.

III. AFSMC SYSTEM

The proposed AFSMC incorporates a sliding mode controller (SMC) with a fuzzy inference system designed to compensate lumped uncertainties. An adaptive tuner

algorithm is developed to adjust the parameters of fuzzy inference system in real time, and also for further confronting the increasing disturbance and uncertainties. The detailed descriptions of each control part of AFSMC are described in the following sections.

A. SMC

For the position tracking objective, we define the tracking error and its derivative:

$$e_y = y - y^*$$
$$\dot{e}_y = v - v^* = x - \dot{y}^*$$

To design the sliding mode control system, the sliding surface can be defined as

$$s = ke_y + \dot{e}_y$$

where k is a positive number. We firstly assume the lumped uncertainty to be bounded, ($|F_d| < \eta \bar{B}_m$), and then choose the Lyapunov candidate as:

$$V_1 = \frac{1}{2} e_y^2$$

The time derivative of V_1 is
$$\dot{V}_1 = e_y(x - \dot{y}^*)$$

Next, let the Lyapunov function candidate be defined as:

$$V_2 = V_1 + \frac{1}{2} s^2 \quad (18)$$

The time derivative of V_2 is
$$\dot{V}_2 = \dot{V}_1 + s\dot{s}$$
$$= e_y s - ke_y^2 + s[-k\dot{e}_y + A_m(s + \dot{y}^* - ke_y) + \bar{B}_m u + F_d - \ddot{y}^*] \quad (19)$$

Considering the equation (19), the sliding mode control law can be obtained as:

$$u_{SMC} = u_{eq} + u_{sw} \quad (20)$$

where

$$u_{eq} = \bar{B}_m^{-1}[-e_y - k\dot{e}_y - A_m(s + \dot{y}^* - ke_y) + \ddot{y}^* - \gamma s] \quad (21)$$
$$u_{sw} = -\eta \, \text{sgn}(s) \quad (22)$$

After replacing control effort in (16) by (20), the following results can be concluded:

$$\dot{V}_2 = -ke_y^2 - \gamma s^2 + sF_d - |s|\eta \bar{B}_m$$
$$\leq -ke_y^2 - \gamma s^2 + |s|(|F_d| - \eta \bar{B}_m)$$
$$\leq -ke_y^2 - \gamma s^2 \leq 0$$

Define the following term

$$W_1(t) = ke_y^2 + \gamma s^2 \leq -\dot{V}_2(t) \quad (23)$$

then

$$\int_0^t W_1(\tau)d\tau \leq -\int_0^t \dot{V}_2(\tau)d\tau = V_2(0) - V_2(t)$$

As $V_1(0)$ is bounded, and $V_1(t)$ is nonincreasing and bounded, then the following result can be concluded:

$$\lim_{t \to \infty} \int_0^t W_1(\tau)d\tau < \infty$$

Since $\dot{W}_1(t)$ is also bounded, $W_1(t)$ is uniformly continuous. By applying Barbalat lemma [14], the following result can be obtained:
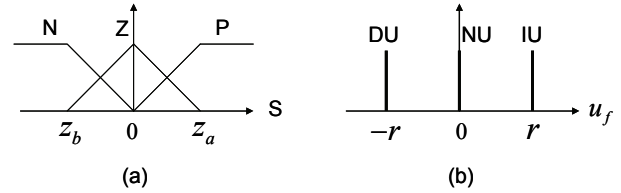

(a)   (b)
Fig. 2. Membership functions of fuzzy sets. (a) Input fuzzy sets for FSMC and AFSMC systems. (b) Output fuzzy sets for FSMC and AFSMC system.

$$\lim_{t \to \infty} W_1(t) = 0$$

The error e_y and $\dot{e}_y$ will converge to zero as $t \to \infty$. Moreover, since the condition $s\dot{s} \leq 0$ holds, a sliding mode is guaranteed on the sliding surface. The SMC system is asymptotically stable whatever there exist system parameters variation, external force disturbance, and friction force.

B. FSMC

Generally, the SMC law can be represented as (20)-(22). The chattering phenomenon induced by the sign function in (22) exists in SMC system, and is hard to apply in actual device. In order to remedy this disadvantage, the concept of fuzzy boundary is introduced to SMC design. The magnitude of the control effort is deeply concerned with the fuzzy boundary. At the same time, this fuzzy boundary is related to the magnitude of uncertainties to pull the error states back to the sliding surface.

Let the sliding surface s be the input linguistic variable of the fuzzy logic, and the control effort u_f be the output linguistic variable. The associated fuzzy sets for s and u_f are expressed as follows:
1) for s [in antecedent proposition]: P (positive), Z (zero), N(negative);
2) for u_f [in consequent proposition]: DU (decreased effort), NU (nominal effort), IU (increased effort)

The fuzzy linguistic rule base involved in the FSMC system can then be summarized as follows:
   Rule (i)   If s is P, then u_f is DU.
   Rule (ii) If s is Z, then u_f is NU.
   Rule (iii) If s is N, then u_f is IU.

The triangular membership functions and center average defuzzification method are adopted in the FSMC system. The membership function shown in Fig. 2. Then, the control effort can be express as follow:

$$u_{FSMC}(t) = u_{eq} + u_f = u_{eq} - r(\omega_1 - \omega_3) \quad (24)$$

where ω_1, ω_2, and ω_3 represent the weighting of rules (i)-(iii), respectively, and $\omega_1 + \omega_2 + \omega_3 = 1$ is hold. We can define the Lyapunov function same as in (17), and its time derivation by using (24) is expressed as

$$\dot{V}_2 = -ke_y^2 - \gamma s^2 + sF_d - r(\omega_1 - \omega_3)\bar{B}_m s$$
$$\leq -ke_y^2 - \gamma s^2 + |s|(|F_d| - r|\omega_1 - \omega_3|\bar{B}_m)$$

Therefore, the inequality

$$r > \frac{|F_d|}{|\omega_1 - \omega_3|\bar{B}_m} \quad (25)$$

Holds, then the sliding condition can be satisfied. Define a function $W_2(t)$ as shown:

$$W_2(t) = ke_y^2 + \gamma s^2 \leq -\dot{V}_2(t)$$

then

$$\int_0^t W_2(\tau)d\tau \leq -\int_0^t \dot{V}_2(\tau)d\tau = V_2(0) - V_2(t)$$

As $V_2(0)$ is bounded, and $V_2(t)$ is nonincreasing and bounded, then one can obtain that:

$$\lim_{t \to \infty} \int_0^t W_2(\tau)d\tau < \infty$$

$\dot{W}_2(t)$ is also bounded, and $W_2(t)$ is uniformly continuous. By applying Barbalat lemma [14], one can obtain the result as follow:

$$\lim_{t \to \infty} W_2(t) = 0$$

That is the error e_y and $\dot{e}_y$ will converge to zero as $t \to \infty$, and the asymptotic stability of FSMC system can be assured under the condition (25).

C. AFSMC

Since the motor moved faster, the more system disturbance induced such as friction force and the motor end effect. That is, the bound of lumped uncertainties could not be found in time in practical application. Therefore, an adaptive tuner algorithm is introduced.

According to (25), we can find an optimal fuzzy boundary r^* to minimize the control efforts and satisfy the sliding condition:

$$r^* = \frac{|F_d|}{|\omega_1 - \omega_3|\bar{B}_m} + \varepsilon \qquad (26)$$

where ε is a small positive constant. In order to estimate the optimal value of the fuzzy boundary, we define estimated error as

$$\tilde{r} = \hat{r} - r^* \qquad (27)$$

where $\hat{r}$ is the estimated fuzzy boundary. Thus, the AFSMC law through (24) can be represented as

$$u_{AFSMC}(t) = u_{eq} + u_{af} = u_{eq} - \hat{r}(\omega_1 - \omega_3) \qquad (28)$$

Based on the control law (28) with the estimated error in (27), a Lyapunov candidate can be chosen as

$$V_3 = V_2 + \frac{1}{2}\frac{1}{\rho}\bar{B}_m\tilde{r}^2 \qquad (29)$$

where ρ is an arbitrary positive constant. One can obtain the time derivative of V_3 is

$$\dot{V}_3 = \dot{V}_2 + \frac{1}{\rho}\bar{B}_m\tilde{r}\dot{\tilde{r}} \qquad (30)$$

After substituting (18), (21), (26)-(28) into (30), the following results can be obtained

$$\dot{V}_3 = -ke_y^2 - \gamma s^2 - s\bar{B}_m[r^*(\omega_1 - \omega_3) - \frac{F_d}{\bar{B}_m}$$

$$+ \hat{r}(\omega_1 - \omega_3) - r^*(\omega_1 - \omega_3)] + \frac{1}{\rho}\bar{B}_m\tilde{r}\dot{\tilde{r}}$$

$$= -ke_y^2 - \gamma s^2 - s(\omega_1 - \omega_3)\bar{B}_m[r^* - \frac{F_d}{\bar{B}_m(\omega_1 - \omega_3)}]$$

$$- s\bar{B}_m(\omega_1 - \omega_3)(\hat{r} - r^*) + \frac{1}{\rho}\bar{B}_m\tilde{r}\dot{\tilde{r}}$$

$$= -ke_y^2 - \gamma s^2 - s(\omega_1 - \omega_3)\bar{B}_m[\frac{|F_d|}{|\omega_1 - \omega_3|\bar{B}_m}$$

$$+ \varepsilon - \frac{F_d}{\bar{B}_m(\omega_1 - \omega_3)}] - s\bar{B}_m(\omega_1 - \omega_3)(\hat{r} - r^*) + \frac{1}{\rho}\bar{B}_m\tilde{r}\dot{\tilde{r}}$$

$$\leq -ke_y^2 - \gamma s^2 - s(\omega_1 - \omega_3)\bar{B}_m\varepsilon - s\bar{B}_m(\omega_1 - \omega_3)\tilde{r} + \frac{1}{\rho}\bar{B}_m\tilde{r}\dot{\tilde{r}}$$

$$= -ke_y^2 - \gamma s^2 - s(\omega_1 - \omega_3)\bar{B}_m\varepsilon + \frac{1}{\rho}\bar{B}_m\tilde{r}\left[\dot{\tilde{r}} - \rho s(\omega_1 - \omega_3)\right]$$

Therefore, the adaptation law for $\hat{r}$ can be designed as

$$\dot{\hat{r}} = \rho s(\omega_1 - \omega_3) \qquad (31)$$

Let $W_3(t) = ke_y^2 + \gamma s^2 + s(\omega_1 - \omega_3)\bar{B}_m\varepsilon \leq \dot{V}_3$, and integrate $W_3(t)$ with respect to time as

$$\int_0^t W_3(\tau)d\tau \leq -\int_0^t \dot{V}_3(\tau)d\tau = V_3(0) - V_3(t) \qquad (32)$$

Since $\dot{V}_3(t)$ is bounded, $V_3(t)$ is nonincreasing and bounded, the following result can be obtained:

$$\lim_{t \to \infty} \int_0^t W_3(\tau)d\tau < \infty$$

Moreover, the function $\dot{W}_3(t)$ is also bounded. Again, by applying Barbalat lemma [14], it can be shown that

$$\lim_{t \to \infty} W_3(t) = 0$$

That is, the sliding surface s will converge to zero as $t \to \infty$. Consequently, the proposed AFSMC scheme assures the system stability and the guaranteed convergence of tracking error to be zero since the condition $s\dot{s} \leq 0$ holds.

IV. EXPERIMENTAL RESULTS

TABLE I
Motor Specification and Parameters

Induction Motor Specification	
Pole pair	2
voltage	230 V
Current	3 A
Pole pitch	0.027 m
Parameter	
M	3.5 kg
D	42.5 kg/s
R_r	8.25 Ω
L_m	0.8 H
L_r	0.96 H
i_{ds}	2.4 A

To implement the proposed scheme, several experiments of position tracking are demonstrated in this section. The motor specifications and parameters of the LIM are listed in Table I. The controller is realized in a pc-based control system for indirect field-oriented LIM drive system using the current-controlled technique. The controller algorithms are carried out using "LabVIEW" package, and are compiled in
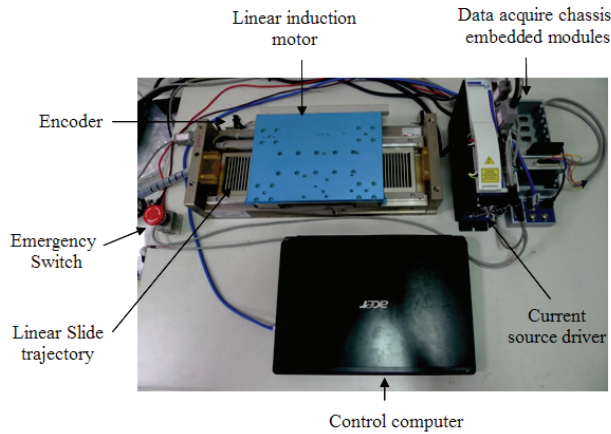
Fig. 3. Photograph of test bench.

the pc-based control computer. The associated photograph of the test bench is depicted in Fig. 3. The control interval of the position control loop is set at 10 ms. The data acquire chassis embedded D/A converter and encoder can provided motor information. The position is measured by a linear encoder with precision $1\mu m$ per pulse, and the D/A converter can fed the control signal to the servo drive card in advance to control the motor. The control parameters, which are considered to achieve the best transient control performance and stability requirement, are chosen as follow:

$$k = 15 \quad \gamma = 15 \quad \eta = 6 \quad r = 6 \quad \rho = 5$$

Consider a position tracking command $y^*(t) = 4\sin 2\pi t$ cm. In this case, we separately implemented the three controllers for comparing their performance. In Figs. 4-6(a), one can find these controllers had well performance in this case. However, the chattering phenomena evidently induced the worse control effort is depicted in Fig. 4(b). The chattering control efforts would deteriorate the motor mechanism and might make the system unstable. An idea of fuzzy boundary is introduced into the SMC scheme for remedying the chattering phenomena and the improvement results are depicted in Figs. 5 and 6. Subsequently, the tracking command was changed as $y^* = 4\sin 6\pi t$ cm. The position responses due to periodic sinusoidal command are depicted in Figs. 7-9(a), and the associated control efforts are depicted in Figs. 7-9(b). From these results, the SMC and FSMC schemes can not adjust boundary to provide compensation control efforts against system uncertainties. Instead, the AFSMC scheme can tune the boundary to alleviate the tracking error and dmonstrate the well tracking performance, as shown in Fig. 9.

V. CONCLUSION

In this study, the design method of backstepping SMC with an adaptive fuzzy boundary layer has been presented. The proposed control scheme incorporates a fuzzy inference system and a dynamic tuner based controller. Moreover, the controller is derived based on the sense of Lyapunov stability theorem to adjust the controller parameter in real-time, and also for further confronting the increasing disturbance and uncertainties. Compared with the SMC and FSMC systems, the proposed AFSMC exhibits robust control performance in dealing with external disturbance and uncertainties by compensating the control effort in real-time. The experimental results show that the AFSMC can outperform the SMC and the FSMC schemes in periodic sinusoidal trajectory tracking performance.

REFERENCES

[1] G. Kang and K. Nam," Field-oriented control scheme for linear induction motor with the end effect," *IEE Proc. Electr. Power Appl.*, Vol. 152, No. 6, pp.1565-1572, 2005.

[2] Jan Jamali, "End effect in linear induction and rotating electrical machines," *IEEE Transaction on Energy Conversion*, Vol. 18, No.3, 2003.

[3] A. Boucheta, I. K. Bousserhane, A. Hazzab, B. Mazari and M. K. Fellah, "Linear induction motor control using sliding mode considering the end effects," in *Proc. 6th International Multi-Conference on Systems, Signals and Devices,* SSD'09, March 23-26, 2009-Djerba, Tunisia.

[4] J. Soltani and M. A. Abbasian, "Robust nonlinear control of linear induction motor taking into account the primary effect," in *Proc. 5th International on Poer Electrons and Motion Control Conference,* Vol. 2, pp. 1-6, 2006.

[5] J. Duncan, "Linear Induction motor - Equivalent-circuit model" *IEE Proc.*, Vol. 130, pt. B, No. 1, pp. 51-57, January, 1983.

[6] F. J. Lin and P.-H Hsu, "Adaptive backstepping sliding mode control for linear induction motor drive," *IEE Proc. Electric Power Applications*, Vol. 149, No. 3, pp.184-194, 2001.

[7] B. K. Bose, "Sliding mode control of induction motor," in *Proc. IEEE-IAS Annu. Meeting*, 1985, pp. 1998.

[8] W. J. Wang and J. Y. Chen, "A new sliding mode position controller with adaptive load torque estimator for an induction motor," *IEEE Trans. Energy Convers.*, Vol. 14, No. 3, pp. 413-418, 1999.

[9] C. T. Lin and C. S. G. Lee, *Neural Fuzzy Systems*. Upper Saddle River, NJ: Prentice-Hall, 1996.

[10] C. M. Liaw and F. J. Lin, "Position control with fuzzy adaptation for induction servomotor" *Proc. Inst. Elect. Eng.─Electr. Power Appl.*, Vol. 142, No. 6, pp. 397-404, 1995.

[11] L. K. Wong, F. H. F. Leung, and P. K. S. Tam, "Lyapunov-function-based design of fuzzy logic controllers and its application on combining controllers," *IEEE Trans. Ind. Electron.*, Vol. 45, No.3, pp. 502-509, 1998.

[12] L. K. Wong, F. H. F. Leung, and P. K. S. Tam, "A fuzzy sliding controller for nonlinear systems," *IEEE Trans. Ind. Electron.*, Vol. 48, No. 1, pp. 32-37, 2001.

[13] A. P. Maulana, H. Ohmori, and A. Sano, "Friction compensation strategy via smooth adaptive dynamic surface control," in *Proc. IEEE CCA Conf. Rec.*, pp. 1090-1095, 1999.

[14] J. J. E. Slotine and W. Li, *Applied Nonlinear Control*. New Jersey: Prentice-Hall, 1991.

[15] L. X. Wang, *A Course in Fuzzy Systems and Control*. Englewood Cliffs, NJ: Prentice-Hall, 1999.
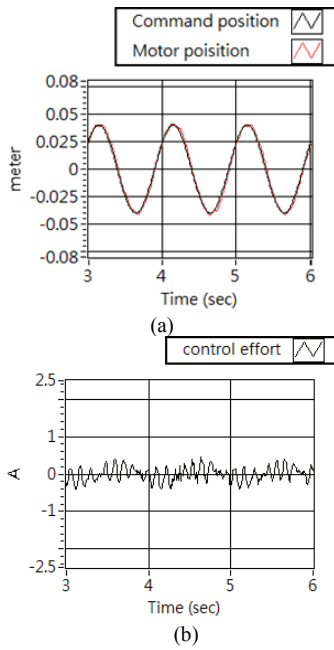
Fig. 4. Experimental results of SMC system. (a) Tracking response. (b) Control effort.
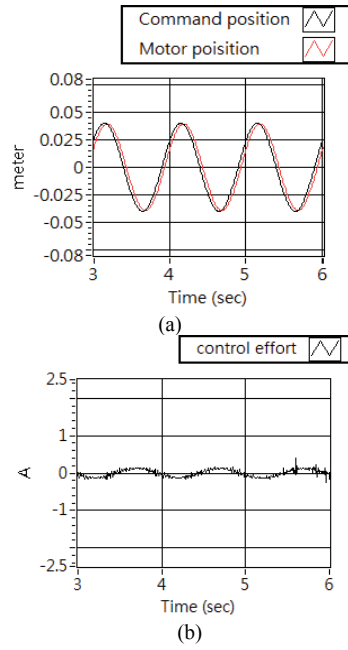

Fig. 5. Experimental results of FSMC system. (a) Tracking response. (b) Control effort.
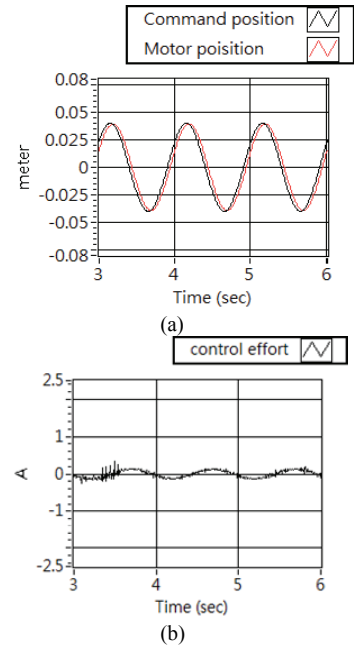

Fig. 6. Experimental results of AFSMC system. (a) Tracking response. (b) Control effort.
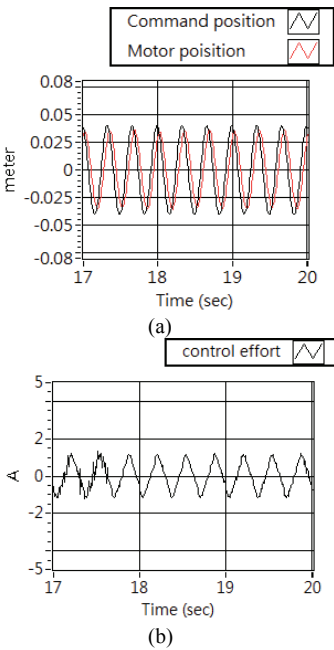

Fig. 7. Experimental results of SMC system. (a) Tracking response. (b) Control effort.
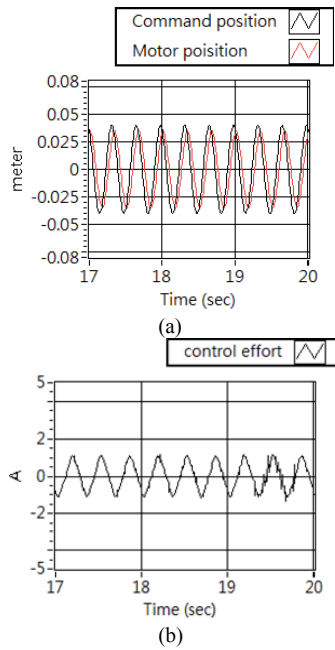

Fig. 8. Experimental results of FSMC system. (a) Tracking response. (b) Control effort.
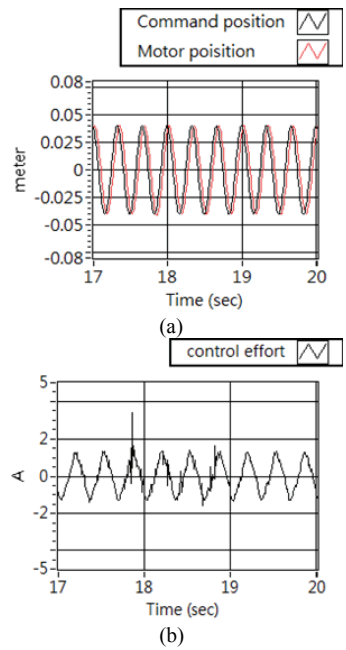

Fig. 9. Experimental results of AFSMC system. (a) Tracking response. (b) Control effort.